IDS'2018 – 21st International Drying Symposium
València, Spain, 11-14 September 2018
DOI: http://dx.doi.org/10.4995/ids2018.2018.7536

Implementation of P-Controller in Computational Fluid Dynamics (CFD) Simulation of a Pilot Scale Outlet Temperature Controlled Spray Dryer

Afshar, S.[a*]; Jubaer, H.[a]; Metzger, L.[b]; Patel, H.[c]; Selomulya, C. [a]; Woo, M.W. [a]

[a]Department of Chemical Engineering, Monash University, Clayton Campus, Victoria 3800, Australia

[b]Department of Dairy Science, South Dakota State University, Brookings, SD 57007, USA

[c]Dairy Foods Research and Development, Land O'Lakes Inc, USA

*E-mail of the corresponding author: sepideh.afshar@monash.edu

Abstract

Most of the CFD simulations of spray dryers reported in the literature utilizes a fixed air inlet temperature numerical framework. In this paper, a numerical framework was introduced to model spray drying as an outlet air temperature controlled process. A P-controller numerical framework was introduced which allows the inlet temperature to be automatically adjusted based on the required outlet temperature set point. This numerical framework was evaluated with a simulation of a two-stage pilot scale spray drying system at the Davis Dairy Plant (South Dakota State University) which is used for commercial contract spray drying operation.

Keywords: *CFD simulation; Multi-Stage Spray Drying; P-Controller*

1. Introduction

Spray drying is a popular unit operation in drying industry in which dry powder can be produced by removing moisture from a liquid material using a hot gas. This is a preferred method where heat sensitive material are used in food and dairy industries. The spray drying involves multiphase flow with heat, mass and momentum transfer between drying gas flow and the discrete phase. Therefore, controlling and designing spray dryers is time-consuming and complicated task particularly where the intent is large-scale production volume [1].

The use of CFD simulations for the design and analysis of spray dryers have been widely reported in the literature [2-5]. A survey of the simulation reported so far revealed that all the simulations employed a fixed inlet conditions (temperature) from which the outlet conditions (temperature) will be predicted. In actual commercial operations, the spray dryer is mainly outlet temperature controlled where the inlet temperature is adjusted (by the control system or sometimes manually), accounting for the evaporation within the chamber, to meet the desired outlet temperature. Such backward computation of the inlet temperature is not trivial in a CFD simulation. Therefore, there is a need for the development of a numerical framework to capture the outlet controlled operation of spray dryers.

In this work, to address this gap in knowledge, a numerical P-Controller was developed for implementation in a CFD simulation of a spray drying system. An industrial scale two-stage spray drying system at Davis Dairy Plant located at South Dakota State University (SDSU) with an external vibrating fluidized bed was modelled where the operation was outlet temperature controlled. In the operation of the SDSU dryer, spraying micellar casein concentrate, the desired temperature of side outlet was set at 82.2^{o}C. Numerical challenges in the development of the P-Controller framework will be further discussed in this paper.

2. Description of the SDSU spray dryer system

Fig. 1 shows the dimensions of the spray drying unit modelled in this paper. The bottom outlet from the chamber leads to the external vibrating fluidized bed as the second stage dryer. The actual mass flow rate of the drying air entering the chamber was not measured or monitored as part of the control system. From the manufacturer's blower performance curve and the measured average pressure at the chamber inlet, the air mass flow rate was determined to be 1.1 kg/s.

The combined operation of the inlet air blower and the main outlet suction blower was used to maintain a negative pressure of approximately 677 Pa (gauge) within the chamber. This negative pressure was measured at approximately the middle elevation of the top conical region of the drying chamber. The bottom outlet pressure was unknown. Simulation of

airflow and particles trajectories ratios between two outlets revealed that the -250 Pa pressure would be a reliable prediction for the bottom outlet [6].

In the startup of the spray dryer, the dryer is firstly heated up with the inlet hot air without spray. At this stage, the automatic system will be manually overridden and a higher temperature, typically at around 161.1-214.4°C to achieve an outlet temperature of 82.2°C, will be used depending on the intended spray rate. Once the dryer reaches the desired outlet temperature, feed spray will be initiated and the automated inlet temperature control will be activated. By intuition, evaporation would have provided cooling to the hot air stream and this would have led to the need for a higher temperature to compensate in maintaining the outlet air temperature. The automatic control system will then increase the inlet air temperature to maintain the outlet temperature at the set point.

3. Modelling approach

The 3D simulations (Fig. 1) of spray dryer with a mesh size of 275764 elements were undertaken using ANSYS Fluent V17.1. [7]. The details of mesh dependency is described in [6]. Boundary condition for air inlet was mass flow inlet that was entered according to the manufacturer's blower air flow specifications (mass flow rate=1.1 kg/s). The walls of the chamber were specified as non-slip insulated wall boundaries. The side outlet (-677 Pa) and the bottom outlet (-250 Pa) were specified as pressure outlets. This approach allowed numerical capturing of the negative pressure within the drying chamber. The pseudo tracer analysis and how to predict the bottom outlet pressure is explained in [6]. Convergence criteria was $1x10^{-3}$ for all scaled residuals.

Transient simulations were undertaken. The Reynolds-time averaged Navier–Stokes conservation equations were used to describe the airflow field. The turbulence in the air was modelled using the standard k–ε model. It has been demonstrated that k–ε model performs much better in transient simulations than steady-state simulations particularly in spray drying systems [8]. For pressure–velocity coupling, the coupled algorithm was used. The transport, turbulence and species equations were discretized using a second-order upwind scheme. Pressure equation was discretized using the PRESTO scheme. A time step size of 0.05s with 10 iterations per time step was sufficient to capture the transient self-sustained central jet flapping behavior of the flow field. This time step size was also adopted by past reports simulating industrial scale spray dryers with inlet air flow of the same magnitude in velocity [9,10]. Particle injection time step sizes were set 0.05s. The "escaping wall" boundary condition was employed at the dryer walls, which assumes that all the particles deposit at the wall upon collision with the wall.

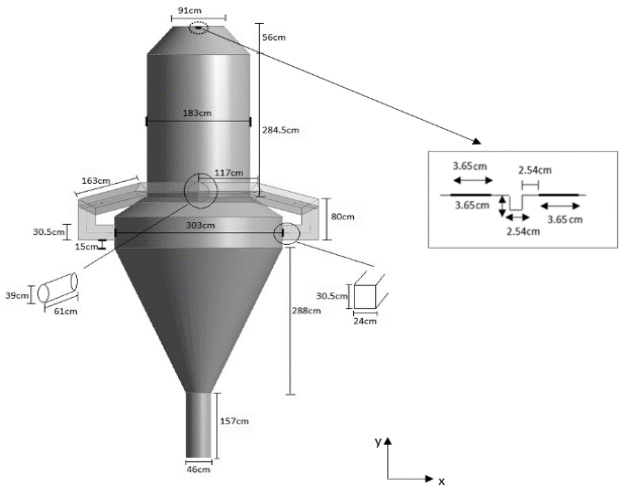

Fig. 1 Dimensions of spray drying chamber

3.1. Equations

Continuity equation is described in Equation (1):

$$\frac{\partial(\alpha_q \rho_q)}{\partial t} + \nabla.\left(\alpha_q \rho_q \vec{v}_q\right) = 0 \quad (1)$$

where q is either gas or solid.

Gas phase-momentum is described in Equation (2):

$$\frac{\partial}{\partial t}(\alpha_g \rho_g \vec{v}_g) + \nabla.\left(\alpha_g \rho_g \vec{v}_g \vec{v}_g\right) = \nabla.\bar{\bar{\tau}}_g - \alpha_g \nabla \mathrm{P} + \alpha_g \rho_g \vec{g} + \beta(\vec{v}_s - \vec{v}_g) \quad (2)$$

Droplet trajectories were captured by the Lagrangian framework. This formulation (Equations (3) to (5)) tracks each discrete droplet individually within the air flow by integrating the motion equations governed by Newton's second law and including the influence of the relevant drag force interaction with the air.

$$\frac{dv_s}{dt} = C_D \frac{18\mu}{\rho_s d} \times \frac{Re}{24}\left(v_g - v_s\right) + g\left(\frac{\rho_s - \rho_g}{\rho_s}\right) \quad (3)$$

$$C_\mathrm{D} = \frac{24}{Re}\left[1 + 0.15(Re)^{0.687}\right] \quad (4)$$

where

$$Re = \frac{\rho_g d\left(v_g - v_s\right)}{\mu_g} \quad (5)$$

The heat transfer model is explained in Equation (6):

$$mC_p \frac{dT_s}{dt} = hA\left(T_g - T_s\right) - \nabla.H_{evap} m_s \frac{dT_s}{dt} \quad (6)$$

The heat transfer coefficient was calculated using Ranz-Marshall equation:

$$Nu = 2 + 0.6Re^{0.5}Pr^{0.33} \quad (7)$$

The distribution of droplet diameters in the spray is assumed to obey the Rosin–Rammler distribution function [11]. The Rosin-Rammler model is given by Equations 8-9:

$$Y_s = e^{-(d/\bar{d})^n} \quad (8)$$

$$n = \frac{ln(-lnY_s)}{\ln(d/\bar{d})} \quad (9)$$

where Y_s is retained mass fraction of particle, d is the particle diameter, $\bar{d}$ is the mean particle diameter and is 394×10^{-7}µm, n is the size distribution parameter and is 2.4. The corresponding maximum and minimum droplet size are taken as 200×10^{-8}µm and 672×10^{-8}µm. User-defined functions (UDFs) in Fluent were developed to describe the shrinkage behavior of particles and Reaction Engineering Approach (REA) models. The particle mixture density was modified using linear shrinkage model [12, 13] (see Equation 10):

$$\frac{d}{d_0} = b + (1+b)\frac{X}{X_0} \quad (10)$$

where d_0 is the initial diameter of the particle/droplet, X_0 is the particle/droplet initial moisture (kg kg^{-1}) on dry basis, and for MCC particles, b is 0.59 [14]. The Reaction Engineering Approach (REA) [15] model for 20 wt% solid content MCC is presented in Equation (11):

$$\frac{\Delta E_v}{\Delta E_{v,e}} = 0.012(X-X_e)^6 - 0.142(X-X_e)^5 + 0.6142(X-X_e)^4 - 1.2944(X-X_e)^3 + 1.483((X-X_e)^2 - 1.0771(X-X_e) + 1.0023 \quad (11)$$

This equation was determined from single droplet measurements in SDSU. The equilibrium moisture content (X_e) for MCC was calculated using Guggenheim-Anderson-de Boer (GAB) model. The constants were taken from [16], and described in Equation 12:

$$X_e = \frac{(0.564 \times RH)}{1 + 6.01RH - 5RH^2} \quad (12)$$

4. Results and Discussion

4.1. Development of the P-Controller numerical scheme

As mentioned in Section 2, the essence of the P-Controller is the continuous adjustment of the inlet temperature based on the outlet temperature relative to the desired outlet temperature set point. In this study, the desired outlet temperature was 82.2°C. In the Fluent framework, the UDF is implemented (hooked) to provide input to the air inlet temperature. The first key aspect of the numerical implementation is that there is a proportional gain parameter embedded into the code which subsequently translates to the step adjustment to the inlet temperature. From trial and error, there was a need to implement an arbitrary maximum possible change to the inlet temperature to ensure stable numerical computation. This limiter to certain extent will be affect by how the simulation is initialized prior to the activation of the P-controller (in case the initial outlet temperature difference relative to the set point is large). The second key aspect to the

numerical implementation is that a response time of the controller was embedded into the framework.

A 'counter' approach was used in the current code corresponding to the enforced number of flow field iterations per time step in the simulation. Both parameters, proportional gain (and the arbitrary limiter) and the response time will affect the simulation time required to achieve a stable air flow outlet temperature. In this work, only the response time was evaluated while keeping the proportional gain parameter constant.

4.2. Evaluation on the effect of different controller response time

Preliminary transient simulations with a fix inlet temperature (without P-controller) showed that characteristic response time of the simulation was approximately 10 seconds. In other words, it takes 10 seconds until the outlet temperature reaches 82.2ºC. Therefore the number of time steps to receive a feedback from P-Controller, between the initial inlet temperature and the calculated outlet temperature was 200, as each time step size was set 0.05 second. The time-step response of 10 seconds was taken as the base study, and the 25s and 35s time-step responses were also investigated. For the brevity, the 25s time-step results were not presented here. Fig. 3 (a-d) shows the inlet and side outlet temperature profiles where time responses are 10s and 35s respectively.

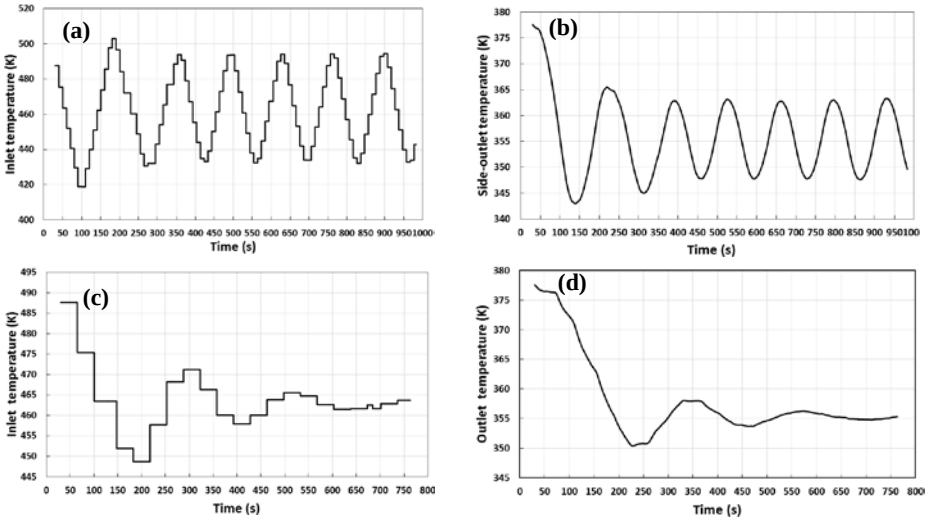

Fig. 3 Temperature profiles (a) inlet temperature: 10s time-step response (b) side-outlet temperature: 10s time-step response (c) inlet temperature: 35s time-step response (d) side outlet temperature: 35s time-step response

As can be seen from Fig. 3(a,b), the temperature profiles kept fluctuating where the time-step response is 10s and the final inlet tempeture is not predictable. However, at 35s time-step responses (Fig.3(c,d)) the temperature profiles were stabilized after approximately

750seconds. The temperature profiles were stabilized after 970 seconds where time-step responses were 25s (For the brevity the figures are not shown here). The measured experimental inlet temperature was 447K, and the predicted CFD inlet temperature was 463K

(Fig. 3(c)). The corresponding error is 3.5%, and it could be due to the uncertainties in other parameters of the simulation such as the atomization parameters or the estimation of the bottom outlet pressure. Nevertheless, this is the first reported attempt in the implementation of the P-Controller for a CFD simulation of spray dryers.

3. Conclusions

CFD simulations of two-stage spray dryer were performed where the inlet temperature was estimated using a P-Controller. The crucial step to estimate the inlet temperature was to predict the proper time-step responses between the inlet and the side-outlet. Comparison of three different time-step responses showed that the longer the time-step responses are the shorter the time required to achieve stabilized temperature profiles. It was found that the time-step response of 35s is adequate to achieve the stabilized temperature profiles. It was proved that the presented P-Controller approach was reasonably able to predict the inlet temperature, however the corresponding error can be due to the uncertainties in obtaining operating parameters from the semi-commercial plant. Future applications of this approach, for faster computation, may require an initial overall black-box mass and energy balance to provide the initial inputs to the dryer from which the P-Controller can then be used for further refinement to the CFD analysis.

Nomenclature

A	Area, [m^2]
b	constant value in Eq. 10
C_D	drag coefficient, [-]
C_p	specific heat capacity, [$J.kg^{-1}.K^{-1}$]
d	diameter, [m]
$\bar{d}$	mean diameter, [m]
ΔE_v	apparent activation energy, [$J.mol^{-1}$]
g	acceleration due to gravity, 9.81 [ms^{-2}]
h	heat transfer coefficient, [Wm^2K^{-1}]
H_{evap}	Heat of evaporation [$J.kg^{-1}$]
m	mass, [kg]
Nu	Nusselt number, [-]
Pr	Prandtl number [-]
P	pressure, [Pa]
Re	Reynolds number, [-]
RH	relative humidity
t	time, [s]
T	Temperature, [K]
v	velocity, [$m\ s^{-1}$]

Greek symbols

α	volume fraction, [-]
μ	dynamic viscosity, [Pas]
ρ	density, [kgm^{-3}]
$\bar{\bar{\tau}}$	stress tensor, [Pa]

Subscripts

e	equilibrium
g	gas phase
s	particle phase

4. References

[1] Mujumdar, A.S.; Handbook of Industrial Drying; Taylor & Francis; Philadelphia, 2007.

[2] Langrish, T.A.G.; Fletcher, D.F. Spray drying of food ingredients and applications of CFD in spray drying. Chemical Engineering and Processing 2001, 40(4), 345-354.

[3] Salem, A.; Ahmadlouiedarab M.; Ghasemzadeh K. CFD approach for the moisture prediction in spray chamber for drying of salt solution. Journal of Industrial and Engineering Chemistry 2011, 17(3), 527-532.

[4] Kieviet, F.G.; Van Raaij, J.; De Moor, P.P.E.A.; Kerkhof, P.J.A.M. Measurement and modelling of the air flow pattern in a pilot-plant spray dryer. Institution of Chemical Engineers 1997, 75, 321-328.

[5] Gabites, J.R.; Abrahamson, J.; Winchester, J.A. Air flow patterns in an industrial milk powder spray dryer. Chemical Engineering Research and Design 2010, 88(7), 899-910.

[6] Afshar, S.; Metzger, L.; Patel, H.; Selomulya, C.; Woo, M.W.; A practical approach to estimate outlet boundary conditions for CFD modelling of industrial multistage spray dryers. International Journal of Drying Technology 2018 (submitted).

[7] ANSYS, Inc. ANSYS®Fluent, in Help system, ANSYS FLUENT Users Guide, Release 17.1; ANSYS, Inc.: U.S.A., 2016.

[8] Harvie, DJE.; Langrish, TAG.; Fletcher, DF. Numerical simulations of gas flow patterns within a tall-form spray dryer. Transations of the Institution of Chemical Engineers 2001, 79 (3), 235–248.

[9] Gabites, JR.; Abrahamson, J.; Winchester, JA. Air flow patterns in an industrial milk powder spray dryer. Chemical Engineering Research and Design 2010, 88 (7) 899-910.

[10] Jin, Y.; Chen, XD. Entropy production during the drying process of milk droplets in an industrial spray dryer. International Journal of Thermal Sciences 2011, 50 (4) 615-625.

[11] P. Rosin, E. Rammler, Journal of the Institute of Fuel, 7 (1933) 29-36.

[12] Lin, S.X.Q.; Chen, X.D. Changes in milk droplet diameter during drying under constant drying conditions investigated using the glass-filament method. Food and Bioproducts Processing 2004, 82(3), 213-218.

[13] Fu, N.; Wai Woo, M.; Selomulya, C.; Chen, X.D. Shrinkage behaviour of skim milk droplets during air drying. Journal of Food Engineering 2013, 116(1), 37-44.

[14] Yang, X.; Xiao, J.; Woo, M.W.; Chen, X.D. Three-Dimensional Numerical Investigation of a Mono-Disperse Droplet Spray Dryer: Validation Aspects and Multi-Physics Exploration. Drying Technology 2015, 33(6), 742-756.

[15] Chen, X.D.; Xie, G.Z. Fingerprints of the drying behaviour of particulate or thin layer materials established using a reaction engineering model. Transactions of the Institution of Chemical Engineers 1997, 77 (A), 21-38.

[16] Foster, K.D.; Bronlund, J.E.; Paterson, A.H.J. The prediction of moisture sorption isotherms for dairy powders. International Dairy Journal 2005, 15(4), 411-418.